Bioorganic & Medicinal Chemistry xxx (2017) xxx–xxx

Contents lists available at ScienceDirect

Bioorganic & Medicinal Chemistry

journal homepage: www.elsevier.com/locate/bmc

Identification of highly potent and orally available free fatty acid receptor 1 agonists bearing isoxazole scaffold

Zheng Li [a,b], Chunxia Liu [b], Wei Shi [b], Xingguang Cai [b], Yuxuan Dai [b], Chen Liao [b], Wenlong Huang [b,c,*], Hai Qian [c,*]

[a] School of Pharmacy, Guangdong Pharmaceutical University, Guangzhou 510006, PR China
[b] Center of Drug Discovery, State Key Laboratory of Natural Medicines, China Pharmaceutical University, 24 Tongjiaxiang, Nanjing 210009, PR China
[c] Jiangsu Key Laboratory of Drug Discovery for Metabolic Disease, China Pharmaceutical University, 24 Tongjiaxiang, Nanjing 210009, PR China

ARTICLE INFO

Article history:
Received 23 November 2017
Revised 16 December 2017
Accepted 22 December 2017
Available online xxxx

Keywords:
Diabetes
FFA1
Lipophilicity
Ligand efficiency
Pharmacokinetic property

ABSTRACT

The free fatty acid receptor 1 (FFA1) is being considered to be a novel anti-diabetic target based on its role in amplifying insulin secretion. We have previously identified several series of FFA1 agonists with different heterocyclic scaffolds. Herein, we describe the structural exploration of other heterocyclic scaffolds directed by drug-like physicochemical properties. Further structure-based design and chiral resolution provided the most potent compound **11** (EC_{50} = 7.9 nM), which exhibited improved lipophilicity ($LogD_{7.4}$: 1.93), ligand efficiency (LE = 0.32) and ligand lipophilicity efficiency (LLE = 6.2). Moreover, compound **11** revealed an even better pharmacokinetic property than that of TAK-875 in terms of plasma clearance, maximum concentration, and plasma exposure. Although robust agonistic activity and PK profiles for compound **11**, the glucose-lowering effects *in vivo* is not ideal, and the exact reason for *in vitro*/*in vivo* difference was worthy for further exploration.

1. Introduction

Type 2 diabetes mellitus (T2DM), a most common type of diabetes, is characterized by impaired insulin secretion and/or sensitization.[1,2] Various available oral insulin secretagogues, such as sulfonylureas, are widely used for the treatment of T2DM.[3] However, these available therapies are often related to side effect of hypoglycemia because insulin secretion induced by them are independent of glucose.[4] Thus, there are unmet needs for new oral insulin secretagogues without the risk of hypoglycemia.

The free fatty acid receptor 1 (FFA1, or GPR40), has emerged as an attractive target in the last decade for the treatment of T2DM.[5] FFA1 is predominantly expressed in the pancreatic β-cell and augments insulin secretion dependent on the levels of glucose, providing a huge advantage of reducing incidence rate of hypoglycemia.[6–8] Moreover, the limited tissue distribution of FFA1 suggests that less possibilities of adverse effects related to FFA1 in other tissues.[9]

As summarized in the most recent review,[10] many literatures have reported structurally diverse FFA1 agonists based on arylalkanoic acids (Fig. 1),[11–18] and the clinical trials were performed to evaluate the potential of TAK-875, LY2881835 and AMG-837 as anti-diabetic agents.[5,10] In addition, the chemical space of FFA1 agonists with different scaffolds has also been explored by our colleagues.[17–24] In particular, the common biphenyl scaffold has been systematically replaced by various heterocycles in our laboratory (eg., compounds **1** and **2** in Fig. 1) to reduce the lipophilicity, and the lipophilicity of candidate is usually related to a higher promiscuity, metabolic instability, and failure rates in research and development.[25–29] Herein, we describe our efforts toward discovering preferable heterocycle scaffold with better drug-like physicochemical properties directed by lipophilicity, ligand efficiency (LE) and ligand lipophilicity efficiency (LLE) (Fig. 2). These efforts ultimately led to the identification of compound **11**, a potent agonist with improved physicochemical properties and excellent pharmacokinetic (PK) profiles.

2. Results and discussion

2.1. Chemistry

The synthesis of heterocycle derivatives **3**–**5** and **8**–**11** is shown in Scheme 1. Compound **2** was synthesized *via* our previous published procedures.[18] The intermediates **3a** or **7a** were provided

* Corresponding authors at: Centre of Drug Discovery, State Key Laboratory of Natural Medicines, China Pharmaceutical University, 24 Tongjiaxiang, Nanjing 210009, China.
E-mail addresses: ydhuangwenlong@cpu.edu.cn (W. Huang), qianhai24@cpu.edu.cn (H. Qian).

https://doi.org/10.1016/j.bmc.2017.12.030
0968-0896/

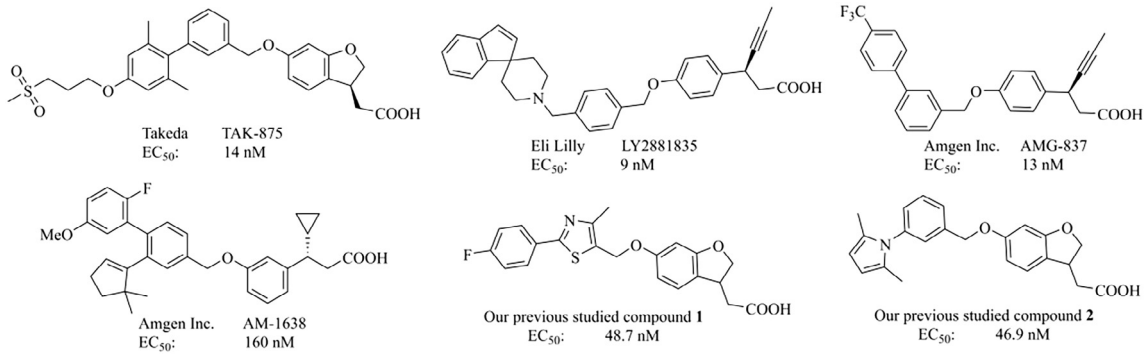

Fig. 1. Synthetic FFA1 agonists.

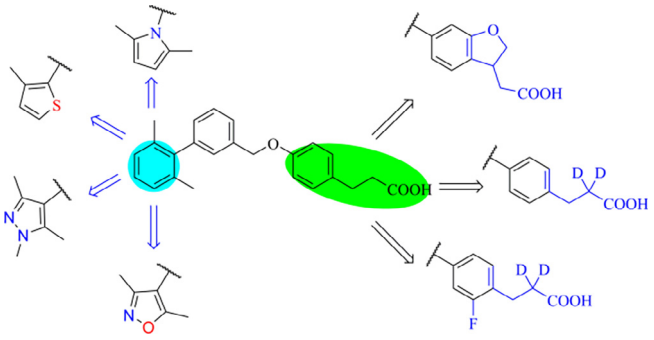

Fig. 2. Design strategy of FFA1 agonists bearing various heterocycles.

by reduction of intermediates **2a** or **6a**, which were prepared from Suzuki-Miyaura cross-coupling of 3-formylphenylboronic acid with commercially available aryl bromide **1a** or **5a** in the presence of $Pd(PPh_3)_4$. The intermediates **3a** or **7a** were treated with thionyl chloride catalyzed by DMF to afford chlorine intermediates **4a** or **8a**. The isoxazole intermediates **12a–d** were synthesized by palladium-catalyzed Suzuki coupling between commercially available isoxazole borate **9a** and appropriate bromobenzene **10a–d**, followed by reduction and chlorination. The dihydrobenzofuran **13a** was prepared *via* previous reported procedures.[11] Williamson ether synthesis of intermediates **4a**, **8a** or **12a–d** with **13a**, followed by basic hydrolysis with lithium hydrate, afforded the desired heterocycle derivatives **3**–**5** and **8**–**10**. A new and simple chiral resolution was developed to convert the racemate **13a** to optically pure **15a** by using R-phenethylamine. Further condensation of intermediate **12b** with **15a**, followed by hydrolysis, furnished the target compound **11**.

The deuterated compounds **6** and **7** were synthesized according to the route summarized in Scheme 2. The key intermediates **17a** and **17b** were afforded by Knoevenagel reaction with Meldrum's acid and 4-hydroxybenzaldehyde **16a–b**, followed by treating with $NaBH_4$. The intermediates **17a** and **17b** were further converted to deuterated **18a** and **18b** by decarboxylation with D_2O and then esterification. Compounds **6** and **7** were synthesized from deuterated intermediates **18a–b** and **12a** by condensation followed by basic hydrolysis.

2.2. FFA1 agonistic activity and structure-based optimization

To counteract the negative factors associated with high lipophilicity, the LE, LLE, and $LogD_{7.4}$ were monitored to screen

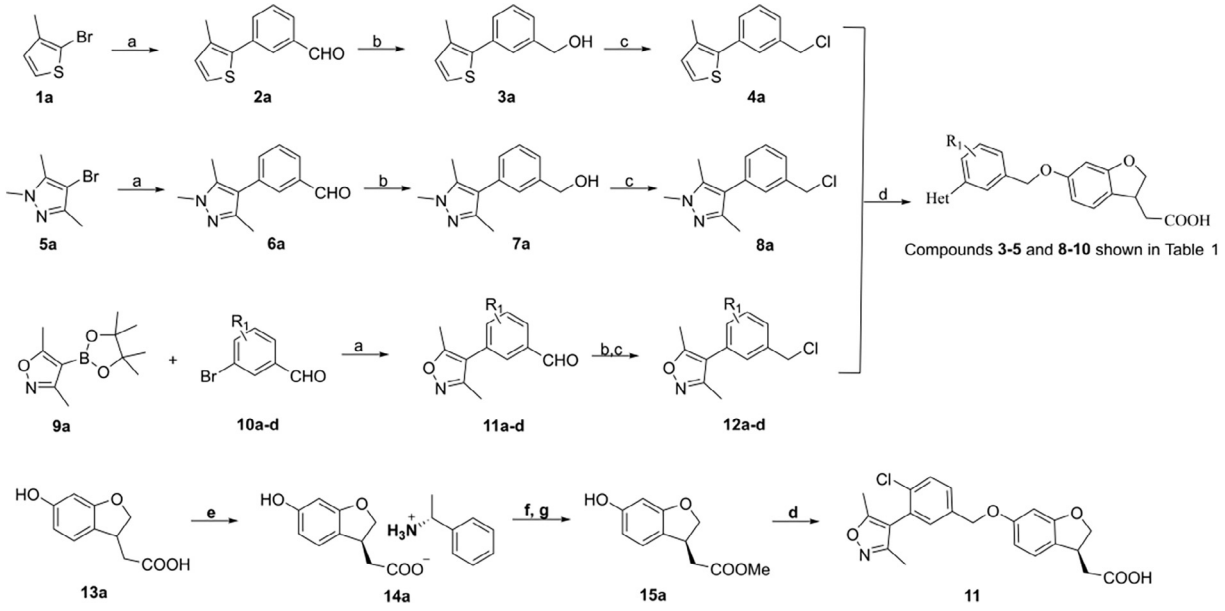

Scheme 1. Synthesis of target compounds **3**–**5** and **8**–**11**. Reagents and conditions: (a) $Pd(PPh_3)_4$, Na_2CO_3, toluene, ethanol, H_2O, 80 °C, 12 h; (b) $NaBH_4$, CH_3OH, THF, 0 °C, 1 h; (c) $SOCl_2$, CH_2Cl_2, DMF, 40 °C, 4 h; (d) **12b** or **13a**, K_2CO_3, KI, acetone, reflux, 12 h; and then $LiOH{\cdot}H_2O$, THF/MeOH/H_2O, rt, 4 h; (e) R-Phenethylamine, acetone, reflux; (f) 1 M HCl; (g) H_2SO_4, MeOH, reflux.

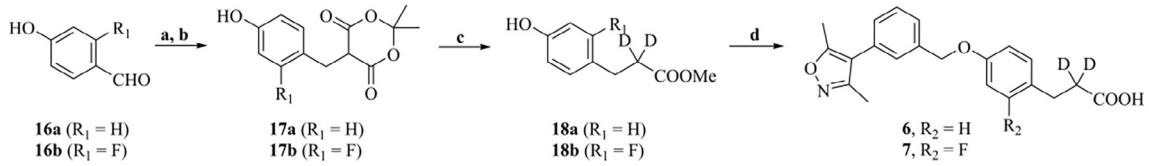

16a (R_1 = H)
16b (R_1 = F)
17a (R_1 = H)
17b (R_1 = F)
18a (R_1 = H)
18b (R_1 = F)
6, R_2 = H
7, R_2 = F

Scheme 2. Synthesis of target compounds **6** and **7**. Reagents and conditions: (a) Meldrum's acid, water, 75 °C, 2 h; (b) $NaBH_4$, r.t.; (c) D_2O, DMF, 100 °C, 12 h, then MeOH, H_2SO_4, reflux, 3 h; (d) **12a**, K_2CO_3, KI, acetone, reflux, 12 h; and then $LiOH{\cdot}H_2O$, THF/MeOH/H_2O, rt, 4 h.

the heterocyclic analogs.[30,31] As shown in Table 1, the thiophene derivative **3** revealed a significantly reduced agonistic activity on FFA1 compared with 2, 5-dimethyl pyrrole analog **2**. As expected, more than 100-fold decrease of lipophilicity (cLogP value: 3.348 *vs* 5.556) was afforded by replacing terminal pyrrole with parazole (compound **4** *vs* **2**) but unfortunately also markedly reduced agonistic activity on FFA1. Gratifyingly, the 3,5-dimethylisoxazole derivative **5** (EC_{50} = 27.5 nM), derived from bioisosterism of parazole analog **4**, exhibited an even stronger potency than compound **2** (EC_{50} = 53.6 nM). Moreover, compound **5** ($LogD_{7.4}$: 1.57) had lipophilicity decreased by more than two log unit than compound **2** ($LogD_{7.4}$: 3.95), and thereby provided a marked advantage on LLE value (6.0 *vs* 3.3). Having identified the preferable 3, 5-dimethylisoxazole scaffold, we next directed efforts to explore the acid head moiety and the deuterated phenylpropionic acid moiety (compound **6** and **7**) was introduced to reduce the β-oxidation of phenylpropanoic acid.[32,33] Interestingly, the *ortho*-fluoro (analog **7**), a substituent increases potency in previous phenylpropionic acid series,[34] turned out to be a slight lower potency than un-substituted analog **6**. This result indicated that the previous structure-activity relationship (SAR) cannot be transferred directly to deuterated series despite the difference between hydrogen and deuterium is quite small.

To better explore the SAR of potent compound **5** series, a molecular docking study was performed using the crystal structure of FFA1 (PDB code: 4PHU). As shown in Fig. 3, the 6-position of

Table 1
In vitro activities of target compounds.

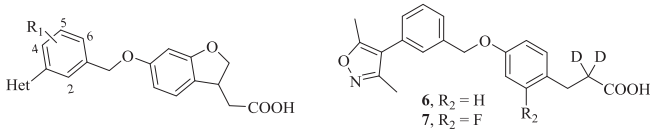

6, R_2 = H
7, R_2 = F

Compd.	R_1	Het	EC_{50} (nM)[a]	cLogP[b]	$LogD^c_{7.4}$	LE (LLE)[d]
TAK-875			31.8	4.697	2.43	0.20 (5.1)
2	H		53.6	5.556	3.95	0.24 (3.3)
3	H		157.1	5.35	ND	
4	H		103.7	3.348	ND	
5	H		27.5	3.212	1.57	0.27 (6.0)
6			38.4	3.395	1.83	0.27 (5.6)
7			45.7	3.678	2.05	0.27 (5.3)
8	4-Cl		18.6	3.706	1.96	0.28 (5.8)
9	6-Cl		39.7	3.956	2.13	0.25 (5.3)
10	6-Me		53.7	3.661	2.07	0.23 (5.2)
11 (S-isomer)	4-Cl	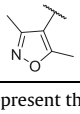	7.9	3.706	1.93	0.32 (6.2)

ND = Not determined. [a] EC_{50} values for FFA1 activities represent the mean of three independent determinations. [b] clogP values were estimated with ChemDraw Ultra, version 12.0. [c] $LogD_{7.4}$ values were determined by shake-flask procedure. [d] LE values were calculated by $-\Delta g = RT\ \ln KD$, presuming $K_D \approx EC_{50}$, and the LLE values were calculated by the formula $pEC_{50} - LogD_{7.4}$.

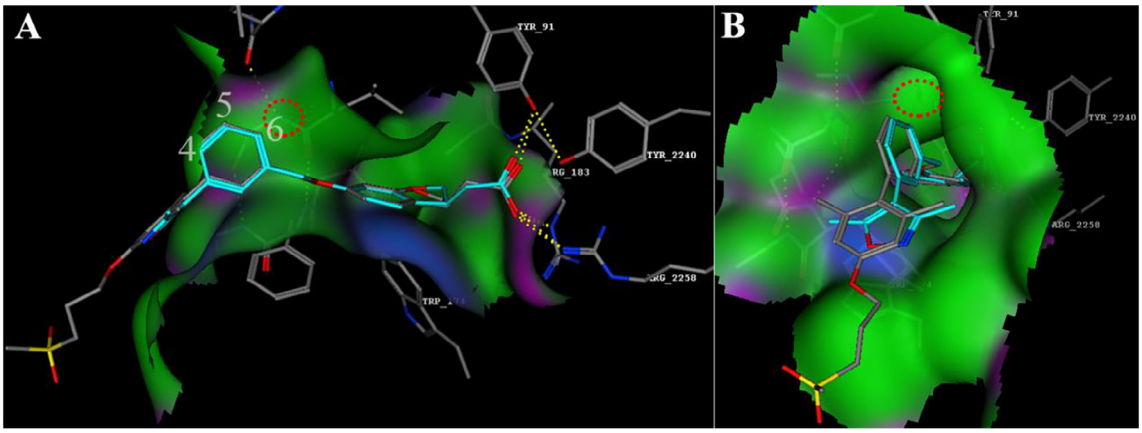

Fig. 3. The frontal view (A) and side-view (B) in docking model of compound **5** (silvery) in crystal structure of hFFA1. Key residues are labeled in white, TAK-875 is represented by gray, and hydrogen bonding interactions are represented by yellow dashed lines, the unoccupied subpocket is highlighted by a red circle.

middle benzene points to an unoccupied hydrophobic subpocket (the red circle), so a better potency might be obtained by occupying this subpocket. Furthermore, the 4-position of middle benzene was exposed to the outside of receptor, which could tolerate a variety of structural optimizations. Therefore, we next focus on incorporating small substituent at the middle phenyl 6-position and 4-position (Table 1). Interestingly, the 4-chlorine derivative **8** exhibited a significant improvement on potency in comparison with compound **5**, but the corresponding 6-position substituted analogs **9** and **10** resulted in a slight reduce of activity. One reasonable explanation is that the steric bulkiness of 6-position substituent might disturb the binding interaction due to the unoccupied subpocket is quite small. Subsequently, we separated the most potent racemic compound **8** by a new chiral resolution with R-phenethylamine and provided the more active (*S*)-enantiomer **11** (EC_{50} = 7.9 nM), which revealed desired lipophilicity ($LogD_{7.4}$: 1.93), LE and LLE values (0.32 and 6.2, respectively). As shown in Fig. 4, compound **11** fitted to the binding site of TAK-875 very well, and the acid moiety was coordinated by hydrogen bonding interaction with Arg183, Arg258 and Tyr91. Moreover, the 4-chlorine of compound **11** was exposed to the outside of FFA1, and could maintain the preferential conformation with 3,5-dimethylisoxazole oriented nearly perpendicularly to middle benzene.

2.3. Effect of selected compounds on glucose tolerance

Based on these positive *in vitro* results, these compounds with considerable potency (compounds **5**, **6**, **8**, **9** and **11**) were selected to evaluate the glucose-lowering effects in mice. As shown in Fig. 5, all of these compounds exhibited glucose-lowering effects to some extent during oral glucose tolerance test (OGTT). Gratifyingly, compounds **6** and **11** (40 mg/kg) significantly lowered the levels of plasma glucose. Notably, the glucose $AUC_{0-120\ min}$ of compound **6** was lower than that of compounds **5** and **8** despite the latter have stronger agonistic activity on FFA1. Besides, the *in vitro* potency of compound **11** (EC_{50} = 7.9 nM) was better than TAK-875 (EC_{50} = 31.8 nM), but the glucose-lowering effect of compound **11** (−26.2%) was still inferior to that of TAK-875 (-37.5%).

2.4. Pharmacokinetic evaluation of compound *11*

In order to determine whether the difference of PK properties is the main reason for their *in vivo* pharmacodynamic differences, the oral PK profiles of TAK-875 and compound **11** were evaluated in fasted SD rats (Table 2). Surprisingly, compound **11** (3 mg/kg) revealed an excellent PK profile in terms of plasma clearance (CL = 18.51 mL/h/kg), maximum concentration (C_{max} = 14.09 μg/mL),

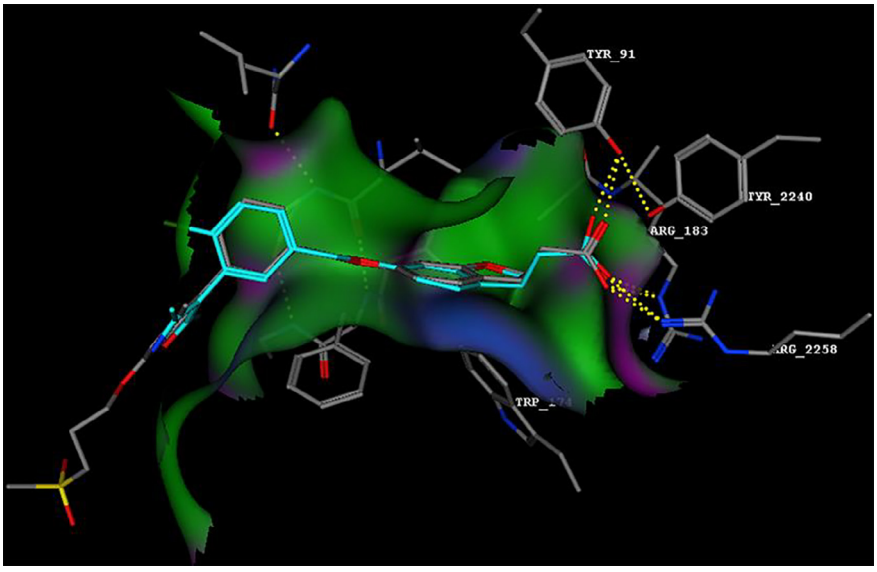

Fig. 4. The docking model of compound **11** in the complex of FFA1 (PDB code: 4PHU). Key residues are labeled in white. Hydrogen bonds are represented by yellow dashed lines. TAK-875 is represented by gray, and compound **11** is represented by silvery.

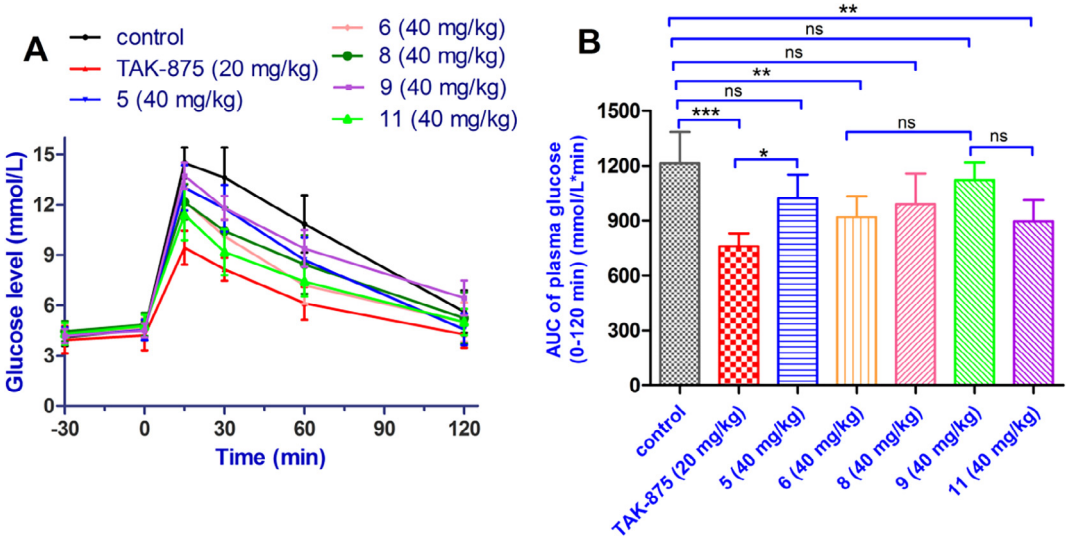

Fig. 5. Effects of selected compounds during OGTT in fasting male ICR mice. (A) represented time-dependent changes of blood glucose levels after oral administration of tested compounds, followed by 3 g/kg oral glucose challenge. (B) represented the $AUC_{0-120min}$ of blood glucose levels. Values are mean ± SD (n = 6 per group). $^{*}p \leq .05$, $^{**}p \leq .01$ and $^{***}p \leq .001$ was analyzed using a one-way ANOVA with Tukey's multiple-comparison post hoc test.

Table 2
PK parameters for TAK-875 and compound **11** in fasted SD rats.

Compd	Dose (po)[a]	CL (mL/h/kg)	C_{max} (μg/mL)	$AUC_{0\text{-}24\ h}$ (μg/mL h)	$T_{1/2}$ (h)
TAK-875	3 mg/kg	37.06 ± 5.81	6.46 ± 1.52	79.52 ± 5.37	4.29 ± 0.56
Compound 11	3 mg/kg	18.51 ± 7.63	14.09 ± 5.28	142.02 ± 35.65	4.65 ± 0.74

[a] po = oral administration. Results are expressed as mean ± SD for four male SD rats (fasted for 12 h) in each group. Test compounds were suspended in 0.5% methylcellulose aqueous solution.

and plasma half-life ($T_{1/2}$ = 4.65 h), which resulted in a more than 1.8-fold drug exposure ($AUC_{0-24\ h}$ = 142.02 μg/mL h) than that of TAK-875 (3 mg/kg, AUC_{0-24h} = 79.52 μg/mL h). In other words, there must be other factors for the *in vivo* pharmacodynamic differences between TAK-875 and compound **11**, such as the differences of drug–target residence time confirmed by Eli Lilly.[35]

3. Conclusion

In the continued SAR study of our previous heterocycle scaffolds represented by compound **2**, we focused especially on improving their drug-like physicochemical properties directed by lipophilicity, LE and LLE. After explored several heterocyclic scaffolds, the potent FFA1 agonists bearing 3, 5-dimethylisoxazole scaffold was identified. Further structure-based optimization and chiral resolution, leading to the discovery of (*S*)-enantiomer **11**, the most potent agonist (EC_{50} = 7.9 nM) in this series with improved lipophilicity ($LogD_{7.4}$: 1.93), LE and LLE values (0.32 and 6.2, respectively). PK evaluation in rats indicated excellent PK profiles and >1.8-fold higher plasma exposure of **11** compared to TAK-875, the most promising candidate in this field. Interestingly, the *in vitro* activity and PK properties of compound **11** were better than TAK-875, but the anti-diabetic effect of compound **11** was inferior to that of TAK-875. Further studies on the identification of *in vitro*/*in vivo* correlation are currently in progress and will be presented in due course.

4. Experimental section

4.1. Chemistry

All starting materials, reagents and solvents were obtained from commercial sources and used without further purification unless otherwise indicated. Column chromatography was carried out on silica gel (200–300 mesh) and monitored by thin layer chromatography performed on GF/UV 254 plates and were visualized by using UV light at 365 and 254 nm. Melting points were measured using a RY-1 melting-point apparatus, which was uncorrected. All of the NMR spectra were recorded on a Bruker ACF-300Q instrument (300 MHz for ^{1}H NMR and 75 MHz for ^{13}C NMR spectra), chemical shifts are expressed as values relative to tetramethylsilane as internal standard, and coupling constants (*J* values) were given in hertz (Hz). LC/MS spectra were recorded on a Waters liquid chromatography-mass spectrometer system (ESI). Elemental analyses were performed by the Heraeus CHN-O-Rapid analyzer. TAK-875 was synthesized via published procedures.[11]

4.1.1. General synthetic procedure for compounds 2a and 6a

The starting materials **1a** or **5a** (1 equiv) and (3-formylphenyl) boronic acid (1 equiv) were dissolved in a mixture of 1 M sodium carbonate aqueous solution (15 mL), EtOH (5 mL) and toluene (15 mL). After nitrogen substitution, $Pd(PPh_3)_4$ (0.05 equiv) was added. The reaction mixture was stirred at 80 °C under nitrogen atmosphere for 12 h. The reaction mixture was cooled, and water (15 mL) was added. The mixture was diluted with AcOEt (15 mL), and the insoluble material was filtered off through Celite. The organic layer of the filtrate was washed with brine, dried over anhydrous sodium sulfate, and concentrated in vacuo. The residue was purified by silica gel column chromatography using a mixture of petroleum ether/ethyl acetate (10:1, v/v) as eluent to afford the desired product **2a** or **6a** as a solid.

*4.1.1.1. 3-(3-methylthiophen-2-yl)benzaldehyde (**2a**).* Yield: 56%; ^{1}H NMR (300 MHz, DMSO-d_6) δ: 10.08 (s, 1H), 7.97 (d, *J* = 1.3 Hz, 1H),

7.88 (d, J = 7.6 Hz, 1H), 7.79 (d, J = 1.3 Hz, 1H), 7.70 (d, J = 7.6 Hz, 1H), 7.54 (d, J = 5.1 Hz, 1H), 7.05 (d, J = 5.1 Hz, 1H), 2.32 (s, 3H).

*4.1.1.2. 3-(1,3,5-trimethyl-1H-pyrazol-4-yl)benzaldehyde (**6a**).* Yield: 48%; ^{1}H NMR (300 MHz, DMSO-d_6) δ: 10.05 (s, 1H), 7.87–7.75 (m, 2H), 7.70–7.56 (m, 2H), 3.72 (s, 3H), 2.24 (s, 3H), 2.15 (s, 3H).

*4.1.2. General synthetic procedure for target compounds **3** and **4***

Step 1: To a solution of **2a** or **6a** (1 equiv) in MeOH (10 mL) and THF (20 mL) was added portionwise sodium borohydride (3 equiv) at 0 °C and the mixture was stirred at 0 °C for 1 h. The reaction mixture was pouring into ice water (10 mL), and extracted with ethyl acetate (3 × 15 mL), the organic fractions were combined, washed with saturated brine (2 × 15 mL) prior to drying over anhydrous sodium sulfate. After filtration and concentrate using a rotary evaporator, the residue was used in next step without further purification. To a solution of the obtained solid (1 equiv) in dichloromethane (20 mL) was slowly added thionyl chloride (6 equiv) and a catalytic amount of DMF at room temperature. After stirring at 40 °C for 4 h, the reaction was concentrated under reduced pressure. The residue was purified by silica gel column chromatography using a mixture of petroleum ether/ethyl acetate (20:1, v/v) as eluent to afford the desired intermediates **4a** or **8a**.

Step 2: To a solution of intermediates **4a** or **8a** (1 equiv) and intermediate **13a** (0.8 equiv) in acetone was added K_2CO_3 (2 equiv) and a catalytic amount of KI at room temperature. The reaction mixture was heated to reflux with stirring overnight. Then the reaction mixture was cooled to room temperature followed by filtration and the filtrate was concentrated under vacuum. The residue was purified by silica gel column chromatography using a mixture of petroleum ether/ethyl acetate (4:1, v/v) as eluent to afford a white solid. To a solution of the obtained solid (1 equiv) in 2:3:1 THF/MeOH/H_2O (18 mL) was added LiOH·H_2O (3 equiv). After stirring at room temperature for 4 h, the volatiles were removed under reduced pressure. The residue was acidified with 1N hydrochloric acid solution, and then filtered and the filter cake was washed with 5 mL of water, dried in vacuum to afford a white powder. The white powder was purified by column chromatography using a mixture of petroleum ether/ethyl acetate (2:1–1:2, v/v) as eluent to afford the target compounds **3** or **4** as white solid.

*4.1.2.1. 2-(6-((3-(3-methylthiophen-2-yl)benzyl)oxy)-2,3-dihydrobenzofuran-3-yl)acetic acid (**3**).* Yield 43%; white solid, m.p. 87–89 °C. ^{1}H NMR (300 MHz, DMSO-d_6) δ: 7.51 (s, 1H), 7.47–7.32 (m, 4H), 7.12 (d, J = 7.8 Hz, 1H), 6.98 (d, J = 5.1 Hz, 1H), 6.56–6.43 (m, 2H), 5.11 (s, 2H), 4.69 (t, J = 9.0 Hz, 1H), 4.31–4.17 (m, 1H), 3.72, 3.68 (dd, J = 13.7, 7.3 Hz, 1H), 2.73, 2.68 (dd, J = 16.6, 5.6 Hz, 1H), 2.48, 2.43 (dd, J = 16.6, 7.3 Hz, 1H), 2.26 (s, 3H). ^{13}C NMR (75 MHz, DMSO-d_6) δ: 173.10, 160.71, 159.06, 137.78, 136.54, 134.23, 133.15, 131.45, 128.86, 127.76, 127.43, 126.67, 126.36, 124.59, 124.16, 122.00, 106.84, 96.80, 77.11, 69.05, 38.85, 37.08, 14.63. ESI-MS m/z: 379.5 [M−1]$^-$. Anal. calcd. For $C_{22}H_{20}O_4S$: C, 69.45; H, 5.30; Found: C, 69.49; H, 5.31.

*4.1.2.2. 2-(6-((3-(1,3,5-trimethyl-1H-pyrazol-4-yl)benzyl)oxy)-2,3-dihydrobenzofuran-3-yl)acetic acid (**4**).* Yield 59%; white solid, m.p. 195–197 °C. ^{1}H NMR (300 MHz, DMSO-d_6) δ: 7.51–7.38 (m, 1H), 7.36–7.24 (m, 2H), 7.20 (d, J = 7.1 Hz, 1H), 7.11 (d, J = 7.8 Hz, 1H), 6.61–6.37 (m, 2H), 5.09 (s, 2H), 4.68 (t, J = 8.9 Hz, 1H), 4.28–4.10 (m, 1H), 3.70 (s, 3H), 3.68–3.64 (m, 1H), 2.72, 2.66 (dd, J = 16.6, 5.2 Hz, 1H), 2.46 (d, J = 9.3 Hz, 1H), 2.19 (s, 3H), 2.11 (s, 3H). ^{13}C NMR (75 MHz, DMSO-d_6) δ: 173.03, 160.66, 159.07, 143.07, 137.37, 136.19, 133.77, 128.55, 128.21, 128.04, 125.17, 124.57, 121.91, 106.87, 96.79, 77.08, 69.18, 40.00, 37.05, 35.69, 12.16, 9.78. ESI-MS m/z: 391.2 [M−1]$^-$. Anal. calcd. For $C_{23}H_{24}N_2O_4$: C, 70.39; H, 6.16; N, 7.14; Found: C, 70.35; H, 6.17; N, 7.15.

The following procedures described the synthesis of compound **12a**, and these procedures can also be applied to the synthesis of compounds **12b–d**.

*Step 1: 3-(3,5-dimethylisoxazol-4-yl)benzaldehyde (**11a**).* To a mixture of 3,5-dimethyl-4- (4,4,5,5-tetramethyl-1,3,2-dioxaborolan-2-yl)isoxazole (0.50 g, 2.2 mmol), 3-bromobenzaldehyde (0.50 g, 2.7 mmol), $Pd(PPh_3)_4$ (0.13 g, 0.12 mmol) and sodium carbonate (0.71 g, 6.7 mmol) in toluene/ethanol/H_2O (35 mL, 3/1/3) was refluxed under nitrogen atmosphere for 24 h. Then the mixture was diluted with saturated ammonium chloride solution and ethyl acetate, and the insoluble material was filtered through Celite. The organic layer of the filtrate was washed with water (25 mL) and brine (25 mL), dried over anhydrous sodium sulfate, and evaporated in vacuo. The residue was purified by column chromatography using a mixture of petroleum ether/ethyl acetate (10:1, v/v) as eluent to afford the desired product **11a** (0.37 g, 77%) as a white solid. ^{1}H NMR (300 MHz, DMSO-d_6) δ: 10.08 (s, 1H), 7.99–7.85 (m, 2H), 7.81–7.63 (m, 2H), 2.43 (s, 3H), 2.25 (s, 3H).

*Step 2: 4-(3-(chloromethyl)phenyl)-3,5-dimethylisoxazole (**12a**).* To a solution of **11a** (0.3 g, 1.49 mmol) in MeOH (10 mL) and THF (20 mL) was added portionwise sodium borohydride (0.17 g, 4.47 mmol) at 0 °C and the mixture was stirred at 0 °C for 1 h. The reaction mixture was pouring into ice water (10 mL), and extracted with ethyl acetate (3 × 15 mL), the organic fractions were combined, washed with saturated brine (2 × 15 mL) prior to drying over anhydrous sodium sulfate. After filtration and concentrate using a rotary evaporator, the residue was used in next step without further purification. To a solution of the obtained solid in dichloromethane (20 mL) was slowly added thionyl chloride (1.06 g, 8.94 mmol) and a catalytic amount of DMF at room temperature. After stirring at 40 °C for 4 h, the reaction was concentrated under reduced pressure. The residue was purified by silica gel column chromatography using a mixture of petroleum ether/ethyl acetate (20:1, v/v) as eluent to afford the **12a** (0.27 g, 82%) as a white solid. ^{1}H NMR (300 MHz, DMSO-d_6) δ: 7.57–7.43 (m, 3H), 7.36, 7.34 (dt, J = 6.9, 1.8 Hz, 1H), 4.82 (s, 2H), 2.41 (s, 3H), 2.23 (s, 3H).

*4.1.3. General synthetic procedure for target compounds **5** and **8–10***

To a solution of **12a–d** (1 equiv) and intermediate **13a** (0.8 equiv) in acetone was added K_2CO_3 (2 equiv) and a catalytic amount of KI at room temperature. The reaction mixture was heated to reflux with stirring overnight. Then the reaction mixture was cooled to room temperature followed by filtration and the filtrate was concentrated under vacuum. The residue was purified by silica gel column chromatography using a mixture of petroleum ether/ethyl acetate (4:1, v/v) as eluent to afford a white solid. To a solution of the obtained solid (1 equiv) in 2:3:1 THF/MeOH/H_2O (18 mL) was added LiOH·H_2O (3 equiv). After stirring at room temperature for 4 h, the volatiles were removed under reduced pressure. The residue was acidified with 1N hydrochloric acid solution, and then filtered and the filter cake was washed with 5 mL of water, dried in vacuum to afford a white powder. The white powder was purified by column chromatography using a mixture of petroleum ether/ethyl acetate (2:1–1:2, v/v) as eluent to afford the target compounds as white solid.

*4.1.3.1. 2-(6-((3-(3,5-dimethylisoxazol-4-yl)benzyl)oxy)-2,3-dihydrobenzofuran-3-yl)acetic acid (**5**).* Yield 61%; white solid, m.p. 105–107 °C. ^{1}H NMR (300 MHz, DMSO-d_6) δ: 7.53–7.30 (m, 4H), 7.10 (d, J = 7.9 Hz, 1H), 6.55–6.42 (m, 2H), 5.10 (s, 2H), 4.66 (t, J = 9.0 Hz, 1H), 4.21–4.12 (m, 1H), 3.68–3.64 (m, 1H), 2.71, 2.66 (dd, J = 16.6, 5.5 Hz, 1H), 2.49–2.40 (m, 1H), 2.36 (s, 3H), 2.19 (s, 3H). ^{13}C NMR (75 MHz, DMSO-d_6) δ: 173.00, 165.13, 160.65, 158.99, 158.04, 137.81, 129.87, 128.94, 128.65, 128.13, 127.92, 126.64, 124.59, 121.99, 117.74, 115.68, 106.84, 96.80, 77.08, 68.98, 40.19,

37.04, 11.22, 10.36. ESI-MS *m/z*: 378.2 $[M-H]^-$. Anal. calcd. For $C_{22}H_{21}NO_5$: C, 69.65; H, 5.58; N, 3.69; Found: C, 69.68; H, 5.57; N, 3.68.

*4.1.3.2. 2-(6-((4-chloro-3-(3,5-dimethylisoxazol-4-yl)benzyl)oxy)-2,3-dihydrobenzofuran-3-yl)acetic acid (**8**).* Yield 31%; white solid, m.p. 168–169 °C. ^{1}H NMR (300 MHz, DMSO-d_6) δ: 7.61 (d, J = 8.2 Hz, 1H), 7.54–7.40 (m, 2H), 7.11 (d, J = 8.2 Hz, 1H), 6.55–6.43 (m, 2H), 5.08 (s, 2H), 4.67 (t, J = 9.0 Hz, 1H), 4.24–4.12 (m, 1H), 3.78–3.59 (m, 1H), 2.67, 2.61 (dd, J = 16.3, 5.4 Hz, 1H), 2.43, 2.38 (dd, J = 16.3, 9.1 Hz, 1H), 2.24 (s, 3H), 2.06 (s, 3H). ^{13}C NMR (75 MHz, DMSO-d_6) δ: 173.57, 166.14, 160.66, 158.71, 158.54, 136.82, 132.51, 131.40, 129.76, 129.24, 128.29, 124.60, 122.54, 113.88, 106.77, 96.83, 77.34, 68.20, 39.95, 37.31, 11.26, 10.11. ESI-MS *m/z*: 412.2 $[M-H]^-$. Anal. calcd. For $C_{22}H_{20}ClNO_5$: C, 63.85; H, 4.87; N, 3.38; Found: C, 63.81; H, 4.88; N, 3.37.

*4.1.3.3. 2-(6-((2-chloro-5-(3,5-dimethylisoxazol-4-yl)benzyl)oxy)-2,3-dihydrobenzofuran-3-yl)acetic acid (**9**).* Yield 45%; white solid, m.p. 127–128 °C. ^{1}H NMR (300 MHz, DMSO-d_6) δ: 7.67–7.49 (m, 2H), 7.40 (d, J = 8.0 Hz, 1H), 7.13 (d, J = 8.1 Hz, 1H), 6.57–6.38 (m, 2H), 5.15 (s, 2H), 4.68 (t, J = 9.0 Hz, 1H), 4.29–4.11 (m, 1H), 3.73–3.64 (m, 1H), 2.71, 2.66 (dd, J = 16.5, 5.5 Hz, 1H), 2.46 (d, J = 9.0 Hz, 1H), 2.30 (s, 3H), 2.17 (s, 3H). ^{13}C NMR (75 MHz, DMSO-d_6) δ: 173.55, 165.98, 161.17, 159.24, 158.46, 135.30, 132.35, 130.96, 130.53, 130.34, 129.42, 125.16, 122.85, 107.16, 97.32, 77.65, 67.29, 40.74, 37.53, 11.70, 10.79. ESI-MS *m/z*: 412.2 $[M-H]^-$. Anal. calcd. For $C_{22}H_{20}ClNO_5$: C, 63.85; H, 4.87; N, 3.38; Found: C, 63.87; H, 4.86; N, 3.38.

*4.1.3.4. 2-(6-((5-(3,5-dimethylisoxazol-4-yl)-2-methylbenzyl)oxy)-2,3-dihydrobenzofuran-3-yl)acetic acid (**10**).* Yield 32%; white solid, m.p. 115–116 °C. ^{1}H NMR (300 MHz, DMSO-d_6) δ: 7.43–7.19 (m, 3H), 7.12 (d, J = 8.7 Hz, 1H), 6.57–6.45 (m, 2H), 5.09 (s, 2H), 4.68 (t, J = 9.0 Hz, 1H), 4.20, 4.17 (dd, J = 8.9, 6.8 Hz, 1H), 3.74–3.67 (m, 1H), 2.72, 2.66 (dd, J = 16.6, 5.6 Hz, 1H), 2.46 (d, J = 9.0 Hz, 1H), 2.34 (s, 6H), 2.17 (s, 3H). ^{13}C NMR (75 MHz, DMSO-d_6) δ: 173.05, 164.86, 160.68, 159.08, 158.08, 135.99, 135.53, 130.62, 128.90, 128.28, 127.15, 124.58, 122.03, 115.62, 106.80, 96.81, 77.12, 67.81, 40.27, 37.07, 18.13, 11.16, 10.34. ESI-MS *m/z*: 392.2 $[M-H]^-$. Anal. calcd. For $C_{23}H_{23}NO_5$: C, 70.21; H, 5.89; N, 3.56; Found: C, 70.25; H, 5.88; N, 3.57.

*4.1.3.4. Methyl (S)-2-(6-hydroxy-2,3-dihydrobenzofuran-3-yl)acetate (**15a**).* A solution of **13a** (9.32 g, 48 mmol) in acetone (50 mL) was heated to reflux, and the solution of R-Phenethylamine (2.91 g, 24 mmol) in acetone (15 mL) was slowly drip into the solution above, then the mixture was allowed to stand at room temperature for 10 h, and a white crystal was precipitate out. The mixture was filtered and the filter cake was treated with 1 M HCl and adjusted pH < 2, which was extracted with ethyl acetate (3 × 20 mL), the organic fractions were combined, washed with saturated brine (2 × 15 mL) prior to drying over anhydrous Na_2SO_4. After filtration and concentrate using a rotary evaporator, the residual white solid was dissolved in acetone (30 mL) and repeated the procedure above for three times, the obtained residue was dissolved in MeOH (15 mL), and then conc. H_2SO_4 (1 mL) was added slowly at ambient temperature. After stirring at reflux for 3 h, the volatiles were removed under reduced pressure. The residue was extracted with ethyl acetate (3 × 25 mL), and the combined organic phases were washed with brine (2 × 15 mL), dried, filtered and the filtrate was concentrated under vacuum. The residue was purified by silica gel column chromatography using a mixture of petroleum ether/ethyl acetate (10:1, v/v) as eluent to afford **15a** (0.32 g, 3.3%) as a white solid, 99.6% ee. ^{1}H NMR (300 MHz, $CDCl_3$) δ: 6.98 (d, J = 8.72 Hz, 1H, ArH), 6.35–6.32 (m, 2H, ArH), 4.83 (brs, 1H, ArOH), 4.76 (t, J = 9.11 Hz, 1H, -OCH_2), 4.26, 4.24 (dd, J = 5.72, 9.11 Hz, 1H, -OCH_2), 3.74–3.84 (m, 1H, ArCH), 3.72 (s, 3H, -OCH_3), 2.73, 2.68 (dd, J = 5.72, 16.41 Hz, 1H, -$COCH_2$), 2.56, 2.51 (dd, J = 9.11, 16.41 Hz, 1H, -$COCH_2$).

*4.1.3.5. (S)-2-(6-((4-chloro-3-(3,5-dimethylisoxazol-4-yl)benzyl)oxy)-2,3-dihydrobenzofuran-3-yl)acetic acid (**11**).* The target compound was prepared as described for compound **5** by using intermediates **15a** and **12b** as starting material. Yield 36%; white solid, 98.2% ee. m.p. 165–166 °C. ^{1}H NMR (300 MHz, DMSO-d_6) δ: 7.63 (d, J = 8.2 Hz, 1H), 7.54–7.41 (m, 2H), 7.11 (d, J = 7.9 Hz, 1H), 6.54–6.42 (m, 2H), 5.09 (s, 2H), 4.68 (t, J = 9.1 Hz, 1H), 4.24–4.16 (m, 1H), 3.78–3.59 (m, 1H), 2.72, 2.66 (dd, J = 16.6, 5.5 Hz, 1H), 2.43, 2.38 (dd, J = 16.3, 9.1 Hz, 1H), 2.25 (s, 3H), 2.07 (s, 3H). ^{13}C NMR (75 MHz, DMSO-d_6) δ: 173.56, 166.13, 160.65, 158.72, 158.54, 136.82, 132.51, 131.40, 129.76, 129.24, 128.29, 124.60, 122.54, 113.88, 106.77, 96.83, 77.34, 68.20, 39.95, 37.31, 11.26, 10.11. ESI-MS *m/z*: 412.1 $[M-H]^-$. Anal. calcd. For $C_{22}H_{20}ClNO_5$: C, 63.85; H, 4.87; N, 3.38; Found: C, 63.88; H, 4.86; N, 3.37.

*4.1.4. General synthetic procedure for intermediates **18a–b***

A mixture of Meldrum's acid (1.1 equiv) and substituted benzaldehyde **16a–b** (1 equiv) in water (10 mL) was stirred at 75 °C for 2 h. After cooling to room temperature the solid product was filtered on Buchner and dried under vacuum. The purification from traces of starting aldehyde, when present, was performed by crystallization with ethanol. The obtained intermediate (1 equiv) was stirred in methanol (20 mL) and $NaBH_4$ was added slowly to keep the temperature between 23 and 28 °C. After stirring for another 15 min, the reaction mixture was acidified (PH: 5–6) with 1N hydrochloric acid solution, and extracted with ethyl acetate (4 × 25 mL), the organic fractions were combined, washed with saturated brine (2 × 15 mL) prior to drying over anhydrous sodium sulfate. After filtration and concentrate using a rotary evaporator, the residue was used in the next step without further purification. To a solution of the obtained solid in DMF (10 mL) was added 0.5 mL D_2O at room temperature. After stirring at 100 °C for 12 h, the mixture was diluted with water (60 mL), and extracted with ethyl acetate (4 × 25 mL), washed with saturated brine (2 × 15 mL) prior to drying over anhydrous sodium sulfate and concentrated in vacuo. The residue was dissolved in MeOH (20 mL), and then conc. H_2SO_4 (2 mL) was added slowly at ambient temperature. After stirring at reflux for 3 h, the volatiles were removed under reduced pressure. The residue was extracted with ethyl acetate (3 × 25 mL), and the combined organic phases were washed with brine (2 × 15 mL), dried and filtered. The residue was purified by silica gel column chromatography using a mixture of petroleum ether/ethyl acetate (10:1, v/v) as eluent to afford the desired product as a solid.

*4.1.4.1. Methyl 3-(4-hydroxyphenyl)propanoate-2,2-d_2 (**18a**).* Yield: 56%; ^{1}H NMR (300 MHz, DMSO-d_6) δ: 9.32 (s, 1H), 7.16 (d, J = 7.9 Hz, 2H), 6.93 (d, J = 7.9 Hz, 2H), 3.63 (s, 3H), 2.74 (s, 2H).

*4.1.4.2. Methyl 3-(2-fluoro-4-hydroxyphenyl)propanoate-2,2-d_2 (**18b**).* Yield: 48%; ^{1}H NMR (300 MHz, DMSO d_6) δ: 9.35 (s, 1H), 7.23–7.15 (m, 2H), 7.05 (d, J = 6.8 Hz, 1H), 3.63 (s, 3H), 2.74 (s, 2H).

*4.1.5. General synthetic procedure for target compounds **6** and **7***

To a solution of **12a** (1 equiv) and intermediate **18a–b** (0.8 equiv) in acetone was added K_2CO_3 (2 equiv) and a catalytic amount of KI at room temperature. The reaction mixture was heated to reflux with stirring overnight. Then the reaction mixture was cooled to room temperature followed by filtration and the filtrate was concentrated under vacuum. The residue was purified by silica gel column chromatography using a mixture of petroleum

ether/ethyl acetate (4:1, v/v) as eluent to afford a white solid. To a solution of the obtained solid (1 equiv) in 2:3:1 THF/MeOH/H_2O (18 mL) was added LiOH·H_2O (3 equiv). After stirring at room temperature for 4 h, the volatiles were removed under reduced pressure. The residue was acidified with 1N hydrochloric acid solution, and then filtered and the filter cake was washed with 5 mL of water, dried in vacuum to afford a white powder. The white powder was purified by column chromatography using a mixture of petroleum ether/ethyl acetate (2:1–1:2, v/v) as eluent to afford the target compounds as white solid.

*4.1.5.1. 3-(4-((3-(3,5-dimethylisoxazol-4-yl)benzyl)oxy)phenyl)propanoic-2,2-d_2 acid (**6**).* Yield 43%; white solid, m.p. 121–123 °C. ^{1}H NMR (300 MHz, DMSO-d_6) δ: 12.08 (brs, 1H), 7.51–7.37 (m, 3H), 7.33 (d, J = 6.6 Hz, 1H), 7.14 (d, J = 8.0 Hz, 2H), 6.93 (d, J = 8.0 Hz, 2H), 5.13 (s, 2H), 2.74 (s, 2H), 2.37 (s, 3H), 2.20 (s, 3H). ^{13}C NMR (75 MHz, DMSO-d_6) δ: 174.25, 165.60, 158.52, 156.99, 138.41, 133.55, 130.40, 129.54, 128.53, 127.15, 116.19, 115.16, 69.27, 29.86, 11.72, 10.86. ESI-MS m/z: 352.1 $[M-H]^-$. Anal. calcd. For $C_{21}H_{19}D_2NO_4$: C, 71.37; H, 6.56; N, 3.96; Found: C, 71.33; H, 6.57; N, 3.95.

*4.1.5.2. 3-(4-((3-(3,5-dimethylisoxazol-4-yl)benzyl)oxy)-2-fluorophenyl) propanoic-2,2-d_2 acid (**7**).* Yield 36%; white solid, m.p. 129–131 °C. ^{1}H NMR (300 MHz, DMSO-d_6) δ: 7.50 (d, J = 6.7 Hz, 1H), 7.46 – 7.42 (m, 2H), 7.33 (d, J = 6.9 Hz, 1H), 7.20 (t, J = 8.7 Hz, 1H), 6.91–6.75 (m, 2H), 5.15 (s, 2H), 2.76 (s, 2H), 2.37 (s, 3H), 2.20 (s, 3H). ^{13}C NMR (75 MHz, DMSO-d_6) δ: 173.52, 165.12, 159.18, 157.92, 137.40, 130.85, 129.98, 128.96, 128.17, 126.74, 115.66, 110.85, 102.44, 102.10, 69.19, 22.95, 11.17, 10.32. ESI-MS m/z: 370.1 $[M-H]^-$. Anal. calcd. For $C_{21}H_{18}D_2FNO_4$: C, 67.91; H, 5.97; N, 3.77; Found: C, 67.94; H, 5.96; N, 3.78.

4.2. Molecular modeling

Docking simulations were performed using MOE (version 2008.10, The Chemical Computing Group, Montreal, Canada). The crystal structure of FFA1 (PDB ID: 4PHU) was downloaded from the Protein Data Bank (PDB). Prior to ligand docking, the structure was prepared with Protonate 3D and a Gaussian Contact surface was draw around the binding site. Subsequently, the active site was isolated and the backbone was removed. The ligand poses was filtered using Pharmacophore Query Editor. The compound structures were placed in the site with Pharmacophore method and then ranked with the London dG scoring function. For the energy minimization in the pocket, MOE Forcefield Refinement was used and ranked with the London dG scoring function.

4.3. Determination of log$D_{7.4}$

In 10 mL glass vial, 40 μL of 10 mM stock solution in DMSO was added 1980 μL phosphate buffer solution (0.01 M, pH = 7.4) and 1980 μL 1-octanol (Sigma), obtaining 100 μM final concentration of the test compounds. The glass vials were shaken at 700 rpm for 24 h and left for 1 h to allow the phases to separate. The 1-octanol phase was pipetted out and diluted ×10 with a mixture of methanol (containing 0.1% formic acid) and MilliQ H_2O (4:1) prior to analysis on HPLC with 60 μL injections. The buffer phase was analyzed directly in 120 μL injections. Each HPLC analysis was performed in duplicates by the method described above. The log$D_{7.4}$ values were calculated by dividing the peak area (mAU * min) at 254 nm of the 1-octanol phase by the corresponding peak area of the buffer phase. Peak areas were corrected for systematic errors using two calibration points per compound per solvent. All test compounds were analyzed in three independent experiments.

4.4. Biological methods

4.4.1. FFA1 agonistic activity (FLIPR Assay)

CHO cells stably expressing human FFA1 were seeded into 96-well plates at a density of 15 K cells/well and incubated 16 h in 5% CO_2 at 37 °C. Then, the culture medium was removed and washed with 100 μL of Hank's Balanced Salt Solution. Subsequently, cells were incubated in loading buffer (containing 2.5 μg/mL fluorescent calcium indicator Fluo 4-AM, 2.5 mmol/L probenecid and 0.1% fatty acid-free BSA) for 1 h at 37 °C. Various concentrations of test compounds or γ-linolenic acid (Sigma) were added into the well and the intracellular calcium flux signals were measured by FLIPR Tetra system (Molecular Devices). The agonistic activities of test compounds on human FFA1 were expressed as $[(A-B)/(C-B)] \times 100$ (increase of the intracellular Ca^{2+} concentration (A) in the test compounds-treated cells and (B) in vehicle-treated cells, and (C) in 10 μM γ-linolenic acid-treated cells). EC_{50} values were obtained with Prism 5 software (GraphPad).

4.4.2. Animals and statistical analysis of the data

8 weeks old SD rats (male, 180–200 g, batch number: SCXK (Jiangsu)2017-0001) and 10 weeks old ICR mice (male, 18–22 g, batch number: SCXK(Jiangsu)2016-0011) were purchased from Comparative Medicine Centre of Yangzhou University (Jiangsu, China), acclimatized for 1 week before experiments. The breeding room was keep on a constant 12 h light/black cycle with temperature at 23 ± 2 °C and relative humidity 50 ± 10% throughout the experimental period. Mice were allowed ad libitum access to standard pellets and water unless otherwise stated, and the vehicle used for drug administration was 0.5% Caboxy Methyl Cellulose aqueous solution for all animal studies. All animal experimental protocols were approved by the ethical committee at China Pharmaceutical University and conducted according to the Laboratory Animal Management Regulations in China and adhered to the Guide for the Care and Use of Laboratory Animals published by the National Institutes of Health (NIH Publication NO. 85-23, revised 2011).

Statistical analyses were performed using specific software (GraphPad InStat version 5.00, GraphPad software, San Diego, CA, USA). Unpaired comparisons were analyzed using the two-tailed Student's t-test, unless otherwise stated.

4.4.2.1. Oral glucose tolerance test. Normal ICR mice 10 weeks old after 1 week adaptation were fasted overnight (12 h), weighted, bled *via* the tail tip, and randomized into 7 groups (n = 6). Mice were administrated orally with a single dose of vehicle, TAK-875 (20 mg/kg), or selected compounds (40 mg/kg) and subsequently dosed orally with 30% aqueous glucose solution (3 g/kg) after half an hour. Blood samples were collected immediately before drug administration (−30 min), before glucose challenge (0 min), and at 15, 30, 60 and 120 min post-dose. The blood glucose was measured by blood glucose test strips (SanNuo ChangSha, China). Data and statistical analyses were performed using GraphPad InStat version 5.00 (GraphPad software, San Diego, CA, USA). General effects were analyzed using a one-way ANOVA with Tukey's multiple-comparison post hoc test.

4.4.2.2. Pharmacokinetic evaluation in SD rats. 8 weeks old normal male SD rats after 1 week adaptation were fasted overnight (12 h), weighted, and randomized into 2 groups (n = 4 for each group). The pharmacokinetic profiles of TAK-875 and compound **11** were determined in fasted male SD rats following single oral dosing (3 mg/kg suspended in 0.5% methylcellulose aqueous solution). At 5, 15, 30, 45 min and 1, 2, 4, 6, 8, 12, 18, 24 h after oral administration, blood samples were collected from tail vein into heparin-containing microcentrifuge tubes. Then centrifuged at 6000 rpm

for 10 min to separate the plasma and stored at −20 °C until analysis. Plasma proteins were precipitated with two volumes of methanol containing an internal standard, mixed by vortexing, and centrifuged at 14,000 rpm for 14 min. The supernatant was diluted and centrifuged again, and 5 μL of supernatant was analyzed by Waters LC-PDA-MS/MS to determine plasma drug levels. Pharmacokinetic profiles were performed using DAS 2.1.1 statistical software program.

Acknowledgement

This study was supported by grants from the National Natural Science Foundation of China (Grants 81673299 and 81273376).

References

1. DeFronzo RA. *Diabetes*. 2009;58:773–795.
2. Danaei G, Finucane MM, Lu Y, et al. Burden Metab risk factors. *Lancet*. 2011;378:31–40.
3. Wajchenberg BL. *Endocr Rev*. 2007;28:187–218.
4. Maedler K, Carr RD, Bosco D, Zuellig RA, Berney T, Donath MY. *J Clin Endocrinol Metab*. 2005;90:501–506.
5. Li Z, Qiu QQ, Geng XQ, Yang JY, Huang WL, Qian H. *Expert Opin Inv Drug*. 2016;25:871–890.
6. Itoh Y, Kawamata Y, Harada M, et al. *Nature*. 2003;422:173–176.
7. Briscoe CP, Tadayyon M, Andrews JL, et al. *J Biol Chem*. 2003;278:11303–11311.
8. Edfalk S, Steneberg P, Edlund H. *Diabetes*. 2008;57:2280–2287.
9. Rayasam GV, Tulasi VK, Davis JA, Bansal VS. *Expert Opin Ther Targets*. 2007;11:661–671.
10. Li Z, Xu X, Huang W, Qian H. *Med Res Rev*. 2017. https://doi.org/10.1002/med.21441.
11. Negoro N, Sasaki S, Mikami S, et al. *Chem Lett*. 2010;1:290–294.
12. Mikami S, Kitamura S, Negoro N, et al. *J Med Chem*. 2012;55:3756–3776.
13. Negoro N, Sasaki S, Mikami S, et al. *J Med Chem*. 2012;55:3960–3974.
14. Hamdouchi C, Kahl SD, Lewis AP, et al. *J Med Chem*. 2016;59:10891–10916.
15. Houze JB, Zhu L, Sun Y, et al. *Bioorg Med Chem Lett*. 2012;22:1267–1270.
16. Brown SP, Dransfield PJ, Vimolratana M, et al. *Chem Lett*. 2012;3:726–730.
17. Li Z, Qiu QQ, Xu X, et al. *Eur J Med Chem*. 2016;113:246–257.
18. Li Z, Pan MB, Su X, et al. *Bioorgan Med Chem*. 2016;24:1981–1987.
19. Li Z, Yang J, Wang X, et al. *Bioorgan Med Chem*. 2016;24:5449–5454.
20. Li Z, Yang JY, Gu WJ, et al. *RSC Adv*. 2016;6:46356–46365.
21. Li Z, Wang X, Xu X, et al. *Bioorgan Med Chem*. 2015;23:6666–6672.
22. Yang J, Li Z, Li H, et al. *Bioorgan Med Chem*. 2017;25:2445–2450.
23. Li Z, Liu C, Xu X, et al. *Eur J Med Chem*. 2017;138:458–479.
24. Yang L, Zhang J, Si L, et al. *Eur J Med Chem*. 2016;116:46–58.
25. Lipinski CA, Lombardo F, Dominy BW, Feeney PJ. *Adv Drug Deliv Rev*. 2012;64:4–17.
26. Christiansen E, Urban C, Grundmann M, et al. *J Med Chem*. 2011;54:6691–6703.
27. Waring MJ. *Expert Opin Drug Dis*. 2010;5:235–248.
28. Keserü GM, Makara GM. *Nat Rev Drug Discov*. 2009;8:203–212.
29. Leeson PD, Young RJ, Med ACS. *Chem Lett*. 2015;6:722–725.
30. Hopkins AL, Groom CR, Alex A. *Drug Discovery Today*. 2004;9:430–431.
31. Leeson PD, Springthorpe B. Nature Rev. *Nat Rev Drug Discovery*. 2007;6:881–890.
32. Li Z, Xu X, Li G, et al. *Bioorgan Med Chem*. 2017;25:6647–6652.
33. Li Z, Liu C, Xu X, et al. *Bioorg Chem*. 2017. https://doi.org/10.1016/j.bioorg.2017.12.012.
34. Sasaki S, Kitamura S, Negoro N, et al. *J Med Chem*. 2011;54:1365–1378.
35. Hamdouchi C, Kahl SD, Patel Lewis A, et al. *J Med Chem*. 2016;59:10891–10916.